

ELECTRON DENSITY IN THE LAVES PHASE $TiMn_2$

M. M. R. COSTA and M. J. M. DE ALMEIDA

Centro FCI (INIC), Departamento de Física da Universidade de Coimbra, 3000 Coimbra — Portugal

(Received 3 October 1986; present form 9 March 1987)

ABSTRACT— Structure factors for the hexagonal Laves phase $TiMn_2$ have been measured by X-ray diffraction, using $Mo-K\alpha$ radiation. The refinement of structural and temperature parameters using a full matrix least-squares technique was carried out.

The main features of the electron density are presented and discussed in terms of Fourier difference maps.

1 — INTRODUCTION

The Laves phase compounds crystallize in three different structures — $MgZn_2$ (C 14), $MgCu_2$ (C 15) and $MgNi_2$ (C 36) — which have been investigated by Friauf [1] and Laves et al. [2]. A review of the crystal and band structures, as well as of the properties of these alloys, has been more recently given by Sinha [3].

The crystalline structure of all Laves phase compounds — which have, in general, a stoichiometric composition AB_2 — can be described in terms of triangular nets of A and B atoms, stacked between a Kagomé net of B atoms. There are several possibilities for the stacking of these layers, giving rise to the three crystallographic structures mentioned above. The difference among them is only in the local symmetry of the nearest neighbours of A and B atoms, their number being the same in all structures.

These alloys have been considered as size factor compounds; the closest packing of the constituent atoms occurs when the

radius ratio R_A / R_B is 1.225. Deviations from this ideal value exist, however, in several Laves phases where R_A / R_B varies between 1.05 and 1.68.

The study of several pseudo-binary systems of these compounds, carried out by Laves et al. [4] and Lieser et al. [5] suggested that a close relationship exists between the crystal structure and the electron concentration, e/a ; in fact, the phase boundaries of the three possible types of structure appear, in all systems investigated, at the same values of e/a . In the alloy $TiMn_2$ the radius ratio is $R_A / R_B = 1.10$. The fact that it deviates from the ideal value suggests that changes in the valences of the constituent elements may occur, which cause the necessary adjustments of atomic volumes so as to preserve the closest possible packing.

This can be investigated by carrying out a careful determination of the electron distribution in this Laves phase. A comparative study of the electron distribution in Laves phase compounds which have a common A element and a B transition metal varying along one line of the periodic table, may be of interest to clarify which of the two factors — atomic size or electron concentration — is dominant in these structures. This work has already been undertaken in our Laboratory on the Laves phases $TiFe_2$, $TiMn_2$ and $TiCo_2$.

2 — EXPERIMENTAL

The Laves phase $TiMn_2$ has the $MgZn_2$ (C 14) hexagonal type of structure, with space group $P6_3/mmc$. The manganese atoms occupy two types of position with different point symmetry; they will be hereafter denoted by Mn(I) — at the origin — and Mn(II) with general coordinates $(x, \bar{x}, 1/4)$.

A single crystal of $TiMn_2$ with approximate dimensions $(0.07 \times 0.06 \times 0.10)$ mm³ was selected from an ingot kindly offered by Dr. M. Nevitt, Argonne National Laboratory, Illinois, U.S.A. The specimen had a somewhat irregular shape which could be approximated by an irregular polyhedron with six faces; Laue photographs confirmed that it was a single crystal.

The diffraction experiment was carried out using a single crystal four-circle diffractometer (CAD4). Lattice parameters were determined by a least-squares standard technique using a set of 25 pre-selected and carefully centered reflections:

$$\begin{aligned} a &= b = (4.8333 \pm 0.0009) \text{ \AA} \\ c &= (7.9384 \pm 0.0011) \text{ \AA} \\ \alpha &= \beta = 90^\circ; \gamma = 120^\circ \end{aligned}$$

These values are in good agreement with those determined by photographic methods and reported by the authors in a previous paper [6]. The integrated intensities of 4915 reflections out to $(\sin \theta) / \lambda = 1.08 \text{ \AA}^{-1}$ were measured in $\omega - 2\theta$ scans, using Mo - K α radiation, monochromated by a graphite crystal. Each reflection hkl was considered to be observed if the corresponding intensity, I_{hkl} , was greater than $3\sigma_{hkl}$, σ_{hkl} being the standard deviation of I_{hkl} .

A set of up to 24 symmetry equivalent reflections was measured for each hkl , in order to evaluate and correct for the effects of absorption and secondary extinction. The intensities of six medium and strong reflections were measured periodically; these were subsequently used as standards to correct the intermediate data for any eventual systematic variation of the main beam intensity.

3 — DATA ANALYSIS

Lorentz and polarization corrections were applied to the reflection data in the usual way.

The empirical absorption correction suggested by North et al [7] brought the integrated intensities of equivalent reflections into agreement within 3%. Least squares refinements including only reflections with $(\sin \theta) / \lambda \geq 0.6 \text{ \AA}^{-1}$ and assuming spherically symmetric scattering factors [8] were carried out in order to refine the scale factor, as well as the positional and thermal parameters for Ti and Mn atoms. The inclusion of only higher order data in these refinements should yield a more reliable value for the scale

TABLE I

	x	y	z	β_{11}	β_{22}	β_{33}	β_{12}
Mn (I)	0	0	0	.00428 (19)	.00428 (19)	.00109 (9)	—
Mn (II)	.82786 (9)	.17214 (9)	1/4	-.00026 (25)	.00985 (27)	.00130 (4)	.00492 (14)
Ti	1/3	2/3	.06398 (13)	.00436 (14)	.00436 (14)	.00144 (7)	—

$S = 0.3347 (24)$ $g = 6.0 (1) \times 10^{-6}$ $R = 2.7 \%$ $R_w = 4.4 \%$

factor, essentially free from correlation with extinction and asphericity effects, as discussed in a previous paper [9].

Structure factors were then calculated for each observed reflection, based on the atomic coordinates and anisotropic temperature factors thus refined. Comparison between calculated and observed structure factors showed that the effect of extinction could not be neglected. Therefore, an extinction coefficient was further refined by least-squares fixing all parameters except the scale factor, and including all the observed reflections.

The results of the above mentioned refinements are shown on table 1. A final set of structure factors was calculated with the refined positions, thermal and extinction parameters, and postulating a spherical distribution of the atomic electrons.

4 — FOURIER ANALYSIS AND RESULTS

Difference Fourier syntheses with coefficients ($SF_{\text{obs}} - F_{\text{calc}}$) were carried out. The results represent the deviations of the observed electron density in $Ti Mn_2$ from the postulated spherical distribution. They can be visualized by drawing difference density maps for several sections of the hexagonal unit cell, as show in figs. 1a) and 1b). The results of Fourier syntheses of the corresponding standard deviations can be seen in figs. 2a) and 2b).

Alternating positive and negative densities (highs and valleys) along vertical lines Ti-Ti are observed on sections parallel to [10.0] at $x = 1/3$. Such oscillations cannot be related to any real charge density effect; their reproducibility will be investigated using another crystal.

The most interesting features, however, are observed on sections parallel to [00.1] at $z = 1/4$: negative contour levels representing a deficiency of about $1.7 e/\text{\AA}^3$ are present along directions joining a pair of Mn (II) atoms (fig. 1a)). This agrees with the contraction of Mn (II)-Mn (II) distances which can be calculated from the results shown on table 2.

The fraction of electrons delocalised from Mn (II)-Mn (II) bonds appears as significant positive contours around the Mn atom on the section parallel to [10.0] at $x = 1/3$ (fig 1b)).

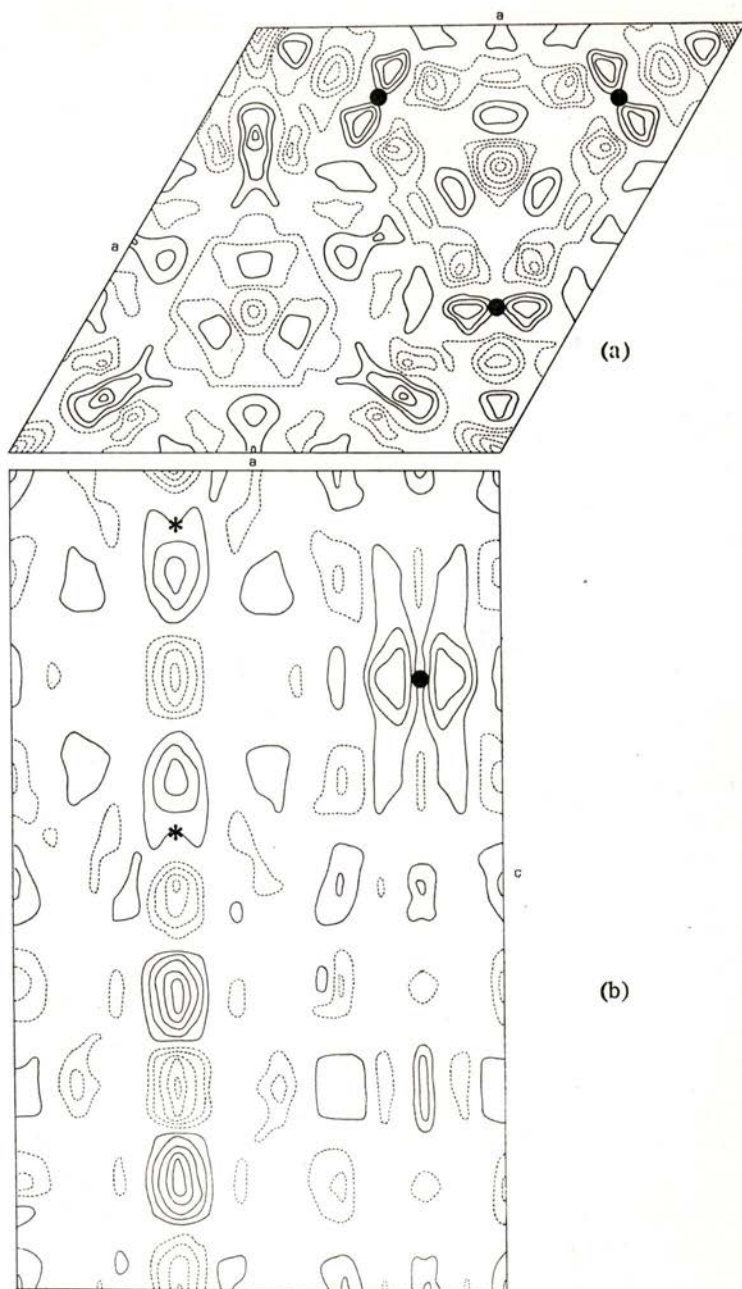


Fig. 1 — Fourier difference maps, $SF_0 - F_c$. Contour levels at $0.43 \text{ e}/\text{\AA}^3$. Broken lines represent negative contours. • Mn atoms; * Ti atoms.

- (a) Section [00.1] of the unit cell at $z = 1/4$
 (b) Section [10.0] of the unit cell at $x = 1/3$

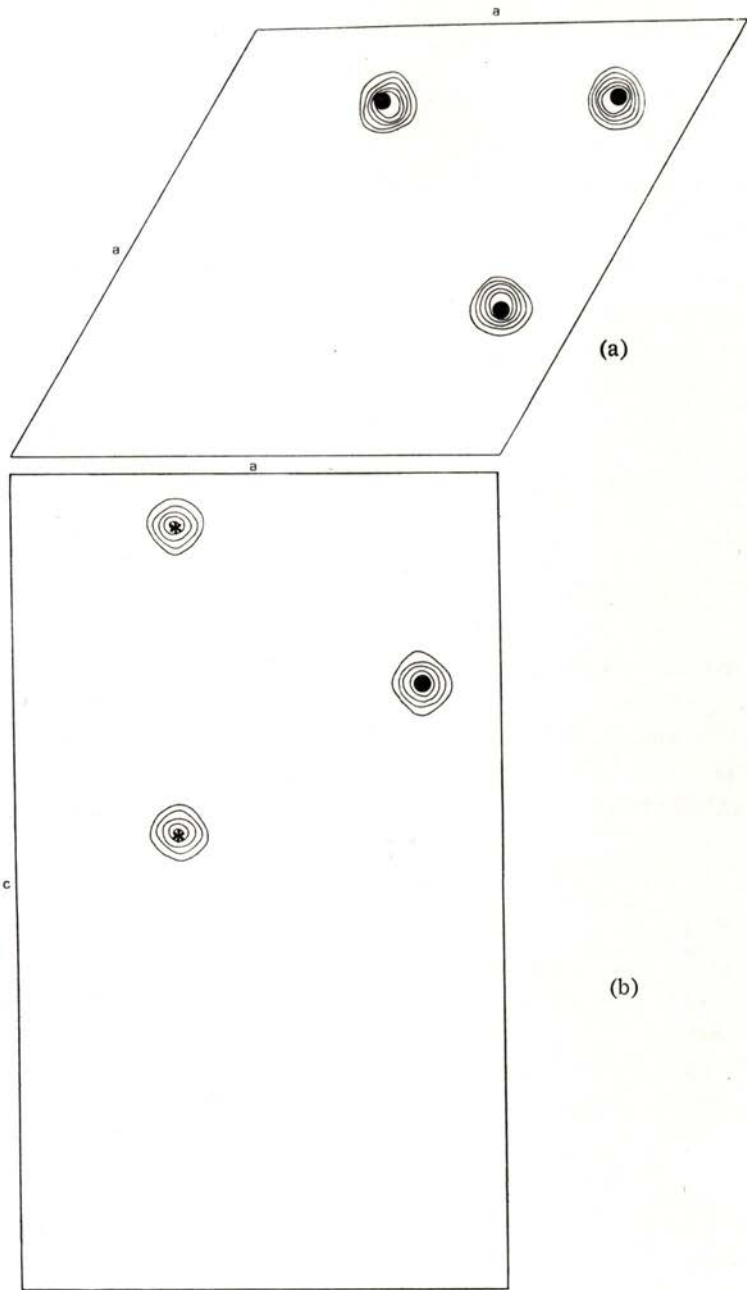


Fig. 2 — Fourier maps representing the distribution of errors.
Contour levels at $0.43 \text{ e}/\text{\AA}^3$.

- (a) Section [00.1] of the unit cell at $z = 1/4$
- (b) Section [10.0] of the unit cell at $x = 1/3$

TABLE 2

Position	Atom	Neighbours	Distance	Atomic radii (CN12)
f	A (Ti)	1 f	2.953 (1)	1.45
		1 f	2.970 (2)	
		6 a	2.836 (2)	
		3 h	2.834 (2)	
a	B (Mn)		2.453 (2)	1.30
h	B (Mn)		2.337 (2)	

We are indebted to the Cultural Service of the German Federal Republic Embassy, the Deutscher Akademischer Austauschdienst (DAAD) and the German Agency for Technical Cooperation (GTZ) for the offer of a CAD4 automatic diffractometer which enabled the experimental work to be carried out.

REFERENCES

- [1] FRIAUF, J. B., *J. Am. Chem. Soc.*, **49**, 3107 (1927).
- [2] LAVES, F. and WITTE, H., *Metallwirtsch. Metallwiss. Metalltech.*, **14**, 645 (1935).
- [3] SINHA, A. K., *Progress in Materials Science*, **15**, 93 (1972).
- [4] LAVES, F. and WITTE, H., *Metallwirtsch. Metallwiss. Metalltech.*, **15**, 840 (1936).
- [5] LIESER, K. H. and WITTE, H., *Z. Metallkd.*, **43**, 396 (1952).
- [6] ALMEIDA, M. J. M., COSTA, M. M. R., ALTE DA VEIGA, L., ANDRADE, L. R. and MATOS BEJA, A., *Portgal. Phys.*, **11**, 219 (1980).
- [7] NORTH, A. C. T., PHILLIPS, D. C. and MATHEWS, F. S., *Acta Cryst.*, **A24**, 351 (1968).
- [8] *International Tables for Crystallography*, vol. III.
- [9] ALMEIDA, M. J. M. and COSTA, M. M. R., *Portgal. Phys.*, **16**, 181 (1985).